Table XI. Positional Parameters for the Atoms of [tmen(2-MeIm)Cu(C_2O_4)Cu(2-MeIm)tmen]$(PF_6)_2$ (3)

atom	x	y	z
Cu	0.28421 (3)	0.15979 (3)	0.18537 (2)
P	0.0802 (1)	0.36055 (9)	−0.31064 (8)
F(1)	0.2407 (5)	0.3841 (4)	−0.3553 (4)
F(2)	−0.0734 (6)	0.3375 (4)	−0.2588 (6)
F(3)[a]	0.156 (1)	0.5053 (6)	−0.241 (1)
F(4)[a]	0.006 (2)	0.216 (1)	−0.375 (1)
F(5)[a]	0.217 (2)	0.313 (1)	−0.2101 (8)
F(6)[a]	−0.064 (1)	0.400 (2)	−0.401 (1)
F(7)[b]	0.176 (2)	0.439 (2)	−0.1841 (8)
F(8)[b]	−0.010 (2)	0.296 (2)	−0.450 (1)
F(9)[b]	0.089 (2)	0.227 (2)	−0.274 (3)
F(10)[b]	0.043 (2)	0.489 (1)	−0.357 (1)
O(1)	0.0116 (2)	0.0355 (2)	0.1502 (1)
O(2)	0.2034 (2)	0.1033 (2)	0.0054 (2)
N(1)	0.3444 (3)	0.2221 (3)	0.3653 (2)
N(2)	0.2609 (3)	0.3490 (2)	0.1615 (2)
N(3)	0.4187 (3)	0.0215 (2)	0.2059 (2)
N(4)	0.6193 (4)	−0.0783 (3)	0.1946 (3)
C(1)	−0.0552 (3)	−0.0196 (2)	0.0421 (2)
C(2)	0.2719 (5)	0.3413 (4)	0.3688 (3)
C(3)	0.3241 (5)	0.4289 (3)	0.2842 (3)
C(4)	0.2527 (6)	0.1207 (4)	0.4212 (3)
C(5)	0.5388 (5)	0.2565 (5)	0.4350 (3)
C(6)	0.0749 (4)	0.3472 (3)	0.0928 (3)
C(7)	0.3745 (5)	0.4096 (3)	0.0939 (4)
C(8)	0.5707 (4)	0.0354 (3)	0.1853 (3)
C(9)	0.4921 (6)	−0.1690 (4)	0.2170 (4)
C(10)	0.3669 (4)	−0.1081 (3)	0.2242 (3)
C(11)	0.6713 (6)	0.1557 (4)	0.1573 (6)

[a] Occupancy 59%. [b] Occupancy 41%.

0.078. At this stage, a difference Fourier map revealing most hydrogen atoms was calculated. The refinement of their positional parameters was carried out by using the thermal parameters of the corresponding heavy atoms at the end of the isotropic refinement. The refinement including all atoms and all observed reflections converged to $R = 0.064$ for 2985 reflections with $I > 4\sigma(I)$ and $2\theta < 50°$. Refined positional parameters for non-hydrogen atoms are listed in Table X.

[tmen(2-MeIm)Cu(C_2O_4)Cu(2-MeIm)tmen]$(PF_6)_2$ (3). As for **1**, space group $P\bar{1}$ was assumed. The Patterson map was used to locate the copper atom. P, O, and N and then C atoms were localized in two steps of alternating least-squares cycles and Fourier synthesis. A refinement with isotropic thermal parameters gave $R = 0.20$ and $R_w = 0.29$. The not surprising disorder of the PF_6^- anion could be only partly resolved from the ensuing difference Fourier map; the introduction of some fluorine atoms in the next cycle of refinement lowered the reliability factors to $R = 0.15$ and $R_w = 0.20$. They were further improved by assigning the Cu, P, O, and N atoms an anisotropic description of thermal motions ($R = 0.10$, $R_w = 0.15$), and the subsequent difference Fourier map was accurate enough to resolve the disorder of PF_6^- and hence to obtain $R = 0.077$ and $R_w = 0.110$. The positions of H atoms were read on the following difference Fourier map and introduced in the least-squares calculations as fixed scatterers with isotropic B factors set equal to the equivalent ones of atoms to which they are bonded. In the last cycle of refinement the highest variable shift/esd ratios were less than 20% for non-fluorine atoms and about 100% for some fluorine atoms. The reliability factors stabilized at $R = 0.038$ and $R_w = 0.057$ for the 3633 observations with $I > 3\sigma(I)$ and 262 variables. The error in an observation of unit weight was 1.98 electrons. Highest peaks in the final difference Fourier map were about $^1/_{15}$th of peaks corresponding to carbon atoms in the final Fourier map. Refined positional parameters for non-hydrogen atoms are listed in Table XI.

Magnetic Measurements. These were carried out with a Faraday type magnetometer equipped with a continuous-flow cryostat working in the temperature range 1.8–300 K. The polycrystalline powder samples weighed about 7 mg. The independence of the susceptibility with regard to the magnetic field was checked at room temperature. Mercury tetrakis(thiocyanato)cobaltate(II) was used as a susceptibility standard. Diamagnetic corrections were estimated as -300×10^{-6}, -300×10^{-6}, and -460×10^{-6} $cm^3\ mol^{-1}$ for **1**, **2**, and **3**, respectively.

Acknowledgment. We are most grateful to E. Philippot and R. Astier of the Université des Sciences et Techniques du Languedoc, Montpellier, for collecting intensities of compound **1**.

Registry No. **1**, 83928-09-0; **2**, 83928-11-4; **3**, 92220-60-5; tmenCu(C_2O_4)·$4H_2O$, 35821-85-3.

Supplementary Material Available: Listings of structure factor amplitudes for compounds **1**–**3** (53 pages). Ordering information is given on any current masthead page.

Contribution from the Department of Chemistry,
Simon Fraser University, Burnaby, British Columbia, Canada V5A 1S6

Structure of the Transition State for Water Exchange on Hexaaquo Divalent Metal Ions

KENNETH E. NEWMAN* and KIM M. ADAMSON-SHARPE

Received October 28, 1983

From a classical electrostatic potential related to that used by Basolo and Pearson, the minimum-energy transition-state structures for water exchange on Ca^{2+}, Mn^{2+}, and Zn^{2+} have been calculated. The results suggest that, in accord with the volumes of activation obtained by high-pressure nuclear magnetic resonance by Merbach and co-workers, at the transition state, metal ions on the right of the periodic table show considerably more extension of their exchanging ligands than those on the left. The potential was also checked by comparing the calculated energies of small alkali-metal ion–water clusters with those obtained by high-pressure mass spectrometry by Dzidic and Kebarle.

Introduction

The development of the dynamics of inorganic reactions owes much to the pioneering book of Basolo and Pearson[1] originally published in 1958. Particularly important was the demonstration that the bond energies of aquo, chloro, and ammine complexes of typically "hard" metal ions could be well calculated in terms of a simple, "soft" charged sphere–polarizable dipole model. Such ideas date right back to the 1920s and have been used both prior to and since Basolo and Pearson's work, but they were particularly successful in demonstrating the soundness of the method by comparing different ligands, different geometries, and different metal ion charges. More recently, Dzidic and Kebarle[2] have measured directly gas-phase alkali-metal ion–water solvation equilibria as a function of temperature by using high-pressure mass spec-

---

[1] Basolo, F.; Pearson, R. G. "Mechanisms of Inorganic Reactions"; Wiley: New York, 1967; Chapter 2.

[2] Dzidic, I.; Kebarle, P. *J. Phys. Chem.* **1970**, *74*, 1466–1474.

0020-1669/84/1323-3818$01.50/0

trometry. They then compared the derived enthalpies of reaction $\Delta H°$ with n (n = 1, 6) for reactions of the form

$$M^+(H_2O)_{n-1} + H_2O \rightleftharpoons M^+(H_2O)_n \quad (1)$$

with those calculated from a classical potential due to Muirhead-Gold and Laidler,[3] which is very similar to that of Basolo and Pearson.[1] The values calculated were considerably higher than the measured ones, and it was concluded that the parameter characterizing the short-range repulsive forces was incorrect. This parameter had been obtained from the second virial coefficients of the isoelectronic noble gases. When this parameter was treated empirically and adjusted so as to make the observed and calculated values for $\Delta H°$ equal when n = 1, there was good agreement for all other values of n. The Basolo and Pearson approach also does include a related approach whereby their function is constrained to have a minimum value at the measured metal ion–ligand bond length.

More recently, quantum-mechanical calculations have been made on metal ion–water clusters, but the approach is not without difficulties. The computational difficulties associated with ab initio calculations of large clusters is immense although one useful approach, that adopted by Clementi, Gorongiu, Jonsson, and Romano[4] is to calculate the energy of interaction of one water molecule with an ion at a large number of different separations and orientations and then to fit this large data set to some form of pseudoclassical potential. This potential is then used to compute the optimum structures and energies of much larger clusters. Less rigorous but more tractable ab inito calculations have been performed such as the mixed electrostatic quantum-chemical (MESQUAC) approach of Rode, Reibnegger, and Fujiwara[5] where the ligands, especially those of outer shells, are represented by their net atomic charges while the central ion is treated fully. Full ab initio calculations are then applied to obtain both optimum configuration and energy.

In addition, molecular dynamics and Monte Carlo calculations have been performed as a means of obtaining information about solution structure and also[6] as a means of assessing the effect of thermal motion on the structure and energy of clusters whose gas-phase energy has been obtained quantum mechanically.

The dynamics of exchange of solvent molecules with a solvated metal ion have also been widely studied but are perhaps less well understood. Basolo and Pearson[1] were able to explain much of the anomalous behavior of solvent exchange and ligand substitution for octahedral complexes of transition-metal ions in terms of the difference in crystal field stabilization energy between octahedral complex and transition state. The only annoying feature of this remarkably successful concept is the inability of the approach to shed light on the mechanism, both associative and dissociative mechanisms showing similar stabilization energies for the anomalous ions.

Shortly after the publication of ref 1, Eigen and co-workers[7] published ultrasonic relaxation studies on a vast variety of metal ion sulfates. For typical octahedral complexes, two relaxation processes were observed, the first being formulated as a diffusion-controlled outer-sphere cation–anion association followed by a much slower interchange whereby the anion replaces a water molecule in the solvation shell. Thus

$$M^{n+}(H_2O)_6 + SO_4^{2-} \rightleftharpoons [M(H_2O)_6{\cdot}SO_4]^{n-2} \rightarrow [M(H_2O)_5SO_4]^{n-2} + H_2O \quad (2)$$

At about the same time, Swift and Connick[8] reported ^{17}O NMR studies on the rate of water exchange for a variety of first-row transition-metal divalent ions. It was the close similarity of the interchange step as measured by Eigen et al. with the solvent exchange rates of Swift and Connick that led to the formulation of what is now known as the Eigen–Wilkins mechanism.[9] This basically stated that the interchange step for substitution reactions was (approximately) independent of the nature of the incoming ligand for all octahedral complexes and was equal to the solvent exchange rate. Subsequently, evidence was found that suggested that Cr^{3+} showed considerable rate sensitivity to the nature of the incoming ligand,[9] and more recently, other trivalent ions have been shown to behave similarly,[10] so much so that some authors[11] have suggested that associative behavior (i.e., dependence on the incoming ligand) is the norm for the trivalent ions, only the very small ions being exceptions. However, with the advent of high-pressure, high-resolution NMR and hence the ability to measure the rates of solvent exchange on transition-metal ions as a function of pressure in order to obtain the volume of activation, doubt has been cast on the dissociative nature of substitution reaction even for divalent octahedral ions. Between Mn^{2+} and Ni^{2+}, the volume of activation changes from negative to positive[12] whereas a dissociative reaction would be predicted to give a positive value always. Some criticism has been leveled at the interpretation of volumes of activation,[13] particularly with regard to the neglect of bond length changes of the nonexchanging ligands although such criticisms have been strongly refuted by both Newman and Merbach[14] and Swaddle.[15] Nevertheless, it is clear that some means of calculating the transition-state structure would be of great interest both as a means of predicting the mechanism of solvent exchange and ligand substitution as well as a means of exploring the problem of the bond lengths of the nonexchanging ligands.

Rode, Reibnegger, and Fujiwara[16] have endeavored to apply their MESQUAC quantum-mechanical calculations to the structure of the transition state for water exchange on various metal ions. They conclude that, since the free energy (strictly the enthalpy) of activation is so much smaller than the calculated bond energies, then the transition state must involve the cooperative nature of the second coordination sphere. Using an interpolation technique between the solvation energies of the first and second solvation spheres, they conclude that the exchange of water on a solvated metal ion occurs via an associative mechanism.

It is the purpose of this work to calculate the structure of the transition state for solvent exchange on octahedral metal ions using the well-established Basolo and Pearson[1] potential. Consideration will be given to the changes that occur in the structure on going from left to right across the periodic table as well the problem of the nonexchanging ligands. The validity of the potential will also be tested by using the gas-phase solvation enthalpies of alkali-metal ions measured by Kebarle et al.

---

(3) Muirhead-Gould, J. S.; Laidler, K. J. *Trans. Faraday Soc.* **1967**, *63*, 944–957.
(4) Clementi, E.; Gorongiu, G.; Jonsson, B.; Romano, S. *J. Chem. Phys.* **1980**, *72*, 260–263.
(5) (a) Rode, B. M.; Reibnegger, G. J. *J. Chem. Soc., Faraday Trans. 2* **1979**, *75*, 178–183. (b) Fujiwara, S.; Rode, B. M. *Bull. Chem. Soc. Jpn.* **1979**, *52*, 3221–3222.
(6) Kistenmacher, H.; Popkie, H.; Clementi, E. *J. Chem. Phys.* **1974**, *61*, 799–815.
(7) Eigen, M. *Pure Appl. Chem.* **1963**, *6*, 97–115.
(8) Swift, T. J.; Connick, R. E. *J. Chem. Phys.* **1962**, *37*, 307–320.
(9) Swaddle, T. W.; Guastalla, G. *Inorg. Chem.* **1968**, *7*, 1915–1920.
(10) Margerum, D. W.; Cayley, G. R.; Weatherburn, D. C.; Pagenkopf, G. K. "Coordination Chemistry"; Martell, A. E., Ed.; American Chemical Society: Washington, DC, 1978; Vol. 2, Chapter 1.
(11) Swaddle, T. W. *Coord. Chem. Rev.* **1974**, *14*, 217–268.
(12) Ducommun, Y.; Newman, K. E.; Merbach, A. E. *Inorg. Chem.* **1980**, *19*, 3696–3703.
(13) Langford, C. H. *Inorg. Chem.* **1979**, *18*, 3288–3289.
(14) Newman, K. E.; Merbach, A. E. *Inorg. Chem.* **1980**, *19*, 2481–2482.
(15) Swaddle, T. W. *Inorg. Chem.* **1980**, *19*, 3203–3205.
(16) Rode, B. M.; Reibnegger, G. J.; Fujiwara, S. *J. Chem. Soc., Faraday Trans. 2* **1980**, *76*, 1268–1274.

Theory

The potential used by Basolo and Pearson[1] may be generalized to any arrangement of central ion and surrounding dipoles by means of the expression (3), where U is the potential

$$U = \sum_i \frac{-q(\vec{\mu}_0 + \vec{\mu}_{\mathrm{ind}})_i \cdot \vec{r}_i}{|\vec{r}_i|^2} + \sum_{\substack{\text{all}\\ \text{pairs}}} \frac{\vec{p}_i \cdot \vec{p}_j - 3(\hat{n}_{ij} \cdot \vec{p}_i)(\hat{n}_{ij} \cdot \vec{p}_j)}{|(\vec{x}_i - \vec{x}_j)|^3} + \sum_i \frac{|(\vec{\mu}_{\mathrm{ind}})_i|^2}{2\alpha} + \sum_i \frac{B}{|\vec{r}_i|^9} \quad (3)$$

energy, $\hat{n}_{ij} = (\vec{x}_i - \vec{x}_j)/|(\vec{x}_i - \vec{x}_j)|$, and $\vec{x}_i$ and $\vec{x}_j$ are the locations of the dipoles $\vec{p}_i$ and $\vec{p}_j$ respectively. $\vec{p}_i = (\vec{\mu}_0 + \vec{\mu}_{\mathrm{ind}})_i$ where $\vec{\mu}_0$ and $\vec{\mu}_{\mathrm{ind}}$ are the permanent and induced dipoles, respectively. q is the charge on the ion, $\vec{r}_i$ is the vector joining the ion and the ith dipole, α is the polarizability of water (1.48 Å^3), and B is the short-range repulsive interaction. The induced dipole is related to the electrostatic field at that point by means of the expression

$$\vec{E}_i = \alpha(\vec{\mu}_{\mathrm{ind}})_i \quad (4)$$

This field is given by

$$\vec{E}_i = \frac{q\vec{r}_i}{|\vec{r}_i|^3} + \sum_j \frac{(\vec{\mu}_0 + \vec{\mu}_{\mathrm{ind}})_i \cdot (\vec{x}_i - \vec{x}_j)}{|(\vec{x}_i - \vec{x}_j)|^{3-}} \quad (5)$$

For highly symmetric arrangements of dipoles, it is clearly not necessary to use such a vector formulation, but for the purposes of this work, the notation proves indispensable. In order to make the above expressions more tractable, it was assumed that both permanent and induced dipoles pointed along the ion–dipole vector. This would imply that the electrostatic field at each dipole was also parallel to that vector. Numerical calculations of the perpendicular component of the field showed that it was small with respect to the total field. Since the electric field is the sum of the fields from the central ion and each of the other dipoles (both permanent and induced), the equations are implicit and must be solved simultaneously. The value of B was obtained according the method of Basolo and Pearson,[1] who constrained the energy to be a minimum at the experimentally determined ion–oxygen bond length. This same value of B was used for the calculation of all the other structures containing that ion. The bond lengths used for the octahedral configuration were given by

$$r/\text{Å} = r_{\mathrm{ir}}/\text{Å} + 1.35 \quad (6)$$

where r_{ir} are the ionic radii as given by Shannon and Prewitt[17] for octahedral coordination. The value of 1.35 was chosen in order that the Ni^{2+}–O distance should be 2.05 Å in accord with the extensive data on this system.[14]

The exchange of water with a hexaaquometal ion is clearly a symmetrical reaction, and hence the reaction profile should also be symmetrical. Providing there are no reactive intermediates formed of either lower or higher coordination number, the transition state should be totally symmetric to the reverse reaction. Assuming that a cis transition state is formed, the structure has to be as given in Figure 1. [A trans transition state turns out to be of much higher energy (see below).] This transition state is characterized by five parameters, viz the bond length of the entering/leaving ligand (r_l), the bond length of the four planar ligands (r_p), the angle of these ligands below the plane (ϕ), the bond length of the ligand trans to the reacting ligands (r_t), and the angle between the entering and leaving ligands (θ).

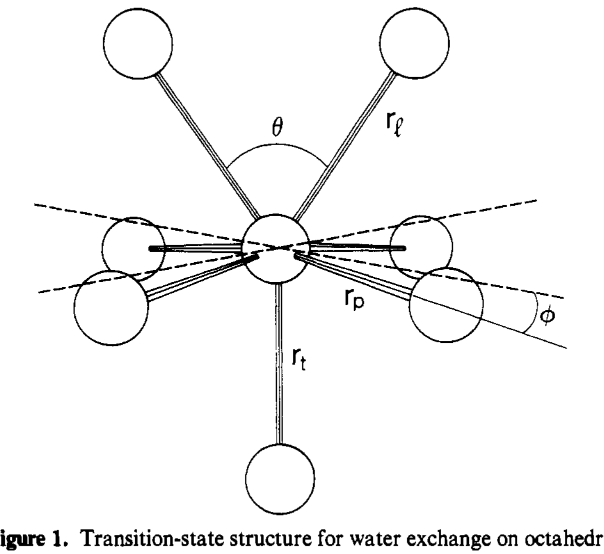

Figure 1. Transition-state structure for water exchange on octahedral hexaaquo divalent metal ions. Also shown are the various bond lengths and angles that define the geometry (see text for details).

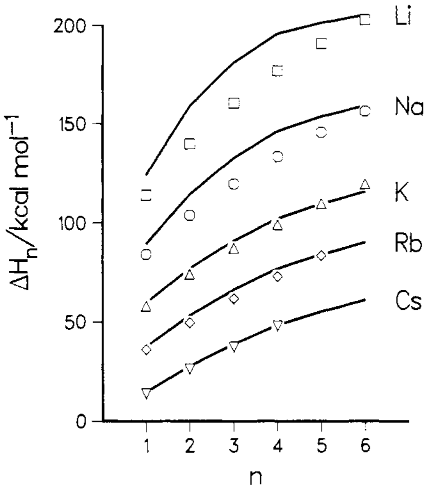

Figure 2. Calculated and observed enthalpies ΔH_n for the reaction $M^+ + nH_2O = M(H_2O)_n^+$ (M = Li to Cs). Successive curves are displaced 20 kcal mol^{-1} vertically for clarity.

Because we wanted to validate this method and also since the results will prove useful in interpreting the transition-state structure, calculations were also performed on one-, two-, three-, and four- (planar and tetrahedral), five- (square-pyramidal and trigonal-bipyramidal), and six- and seven- (pentagonal-bipyramidal) coordinate structures as well as the transition state. The calculations of the transition state proved very useful in this regard since, by setting r_p to a very large value, θ to 60°, and r_l to equal r_t, one is in effect calculating the planar, three-coordinate structure. This calculation can be verified by a direct hand calculation of the same structure. In this way, all aspects of the transition-state calculation can be checked.

The energies of the various structures were minimized with respect to the various bond lengths and angles by using nonlinear least-squares approaches. Two routines were used: the Numerical Algorithms' Group E04JBF and Cern's MINUIT. In general, the two programs gave identical results although for the more complex calculations, MINUIT was far superior.

Results and Discussion

In order to validate the procedure, calculations were made on alkali-metal ions with between one and six water molecules so that comparison could be made with the experimental work of Kebarle et al.[2] It was observed that the calculated bipyramidal structures consistently gave lower energies than the square-planar ones, and for simplicity, this structure was

---

(17) Shannon, R. D.; Prewitt, C. T. *Acta Crystallogr., Sect. B: Struct. Crystallogr. Cryst. Chem.* **1969**, *B25*, 925–946.

Table I. Energies and Structures of both Octahedral Ground States and Transition States for Water Exchange on Ca^{2+}, Mn^{2+}, and Zn^{2+}

	$-E$/ kcal mol	r_p/r_0	r_t/r_0	r_l/r_0	θ/ deg	ϕ/ deg	bond breaking/ %
				Octahedral Ground State			
Ca	265.3	1[a]					
Mn	317.0	1[b]					
Zn	342.6	1[c]					
				Transition State			
Ca	269.7	1.011	1.017	1.090	69.3	6.6	35
Mn	316.0	1.000	1.016	1.157	65.3	4.0	48
Zn	339.3	0.988	1.002	1.289	63[d]	0.0	72

[a] $r_0 = 2.35$ Å. [b] $r_0 = 2.17$ Å. [c] $r_0 = 2.095$ Å. [d] Fixed value.

chosen with all bond lengths constrained to be equal. The comparison between theory and experiment is shown in Figure 2. It would appear that the theory may slightly overestimate the curvature of the plot, but on the whole, the agreement was very satisfactory. As was pointed out earlier,[14] the reason for the curvature, i.e. the nonadditivity of enthalpies of successive solvation steps, is the existence of important ligand–ligand interactions and it would appear likely that this approach may slightly overestimate this contribution. The results agree well with the quantum-mechanical calculations of Kistenmacher, Popkie, and Clementi,[6] who used a Hartree–Fock two-body potential and two different Hartree–Fock approaches where pairwise additivity is not assumed, one using a large basis set and the other using a minimal set. In addition they performed a Monte Carlo simulation using the two-body potential in order to assess the effect of thermal motion on their calculations. As mentioned above, the classical calculations of Kebarle et al.,[2] which contain no adjustable parameters, do not agree with the experimental values unless certain constraints are built in. The energy obtained for $n = 1$ also agrees well with the minimum energy obtained from a classical trajectory study for a water molecule impinging on a Li^+ ion performed by Hase and Feng.[18] These authors used the two-body potential developed by Clementi et al.[6] In addition, the computed bond lengths agree well with the quantum-mechanical calculations although this is a far less stringent test. We are thus led to believe that our classical calculations can be used to obtain reliable values for the energies of small metal ion–water clusters.

With the validity of the method proved for the alkali-metal ions, calculations were undertaken on various first-row divalent d metal ions. In order to eliminate (for the present) the added complexity of ligand field effects, this work was limited to Ca^{2+}, Mn^{2+}, and Zn^{2+}. The results of the calculations of four- to seven-coordinate structures as well as that of the transition state are summarized in Table I. Full optimization of angles and all nonequivalent bond lengths was performed. For the very small Zn^{2+} ion, θ was fixed at 63° since with θ as a variable the bond lengths of the reacting ligands became very large as did θ, so that the reacting ligands were located beyond and behind the planar ligands, minimizing their energy by a direct dipole–dipole attraction. In aqueous solution, this would be unlikely to occur since the reacting ligands would then be subject to large interactions with the second solvation shell. Regardless of the validity of fixing θ at 63°, it is very clear that the Zn^{2+} ion is behaving in a manner different from that of the other two ions. It is clear from Table I that the bond length changes of the nonreacting ligands going from the octahedral to the transition-state structure are very small, a maximum of but 2%. An equally valid structure for the transition state from the viewpoint of microscopic reversibility is the pentagonal bipyramid, but it was shown that the energy is much higher and also the reacting ligands, i.e. the trans ligands, are more strongly bound than the axial ones. It is thus extremely unlikely that the trans ligands would be the ones to exchange, and hence it cannot be the transition state.

Concepts of bond energy are extremely useful in spite of the difficulties associated with the idea that successive breaking of initially identical bonds does not require identical amounts of energy. In order to explore the problem of bond energies in more detail and to see whether the bond energies are, in any sense, additive, the data in Table I were analyzed by means of

$$U = \sum_i a/r_i^m \tag{7}$$

where a and m are parameters to be optimized for each ion. The summation is taken over all ligands. The quality of the fit is remarkably good; variation between the tabulated value and that predicted by eq 7 was always less than 1 kcal/mol. Interestingly, the only structure for which the fit was poor was the Zn^{2+} transition-state structure with θ unconstrained, the structure that was rejected as being physically unreasonable. Clearly, eq 7 cannot take into account the large dipole–dipole attraction that is clearly not a direct function of distance from the ion.

The interesting consequence of eq 7 is that one may calculate from the degree of extension of the reacting ligands going from octahedral to transition state the extent of bond breaking without the added complication of changes in the other nonreacting bonds. The results are that for Ca^{2+} the bonds are 35% broken at the transition state, for Mn^{2+} 48% broken, and for Zn^{2+} 72% broken. These results clearly support the hypothesis developed from the volume of activation studies[12] that there is a gradual change of mechanism that does occur on going from left to right across the periodic table. It is interesting to note that for Mn^{2+} the existence of two bonds approximately 50% formed at the transition state is clearly manifest in the close similarity between the energies of the octahedral ground state and the transition state.

It is clear that the calculated changes in transition state are largely determined by changes in the crystal radii. For the trivalent ions, however, the available volume of activation data suggests that Cr^{3+} reacts in a more associative manner than Fe^{3+} [19] and yet Cr^{3+} is slightly smaller than Fe^{3+}. Further work is in progress to extend the calculations to ions where crystal field effects are important and also to study changes in the steepness of the repulsive term, which are likely to affect bond compressibilities, in order to resolve these problems.

The calculations described above refer to a hypothetical gas-phase reaction, and there are clearly problems in extrapolating to the liquid phase. The process discussed may be formulated as

$$H_2O(g) + M(H_2O)_6(g) \xrightarrow{\Delta E} [M(H_2O)_7]^{\ddagger} \tag{8}$$

from which it is clear that, in terms of transition-state theory, the liquid-phase activation enthalpy $\Delta H^{\ddagger}$ is given by

$$\Delta H^{\ddagger} = \Delta E + \Delta H_s(\text{ts}) - \Delta H_s(\text{oct}) + \Delta H_v \tag{9}$$

where ΔH_s(ts) and ΔH_s(oct) refer to solvation enthalpies of the transition state and the ground state, respectively, and ΔH_v is the enthalpy of evaporation of water. When the ΔH_s terms are neglected, the activation enthalpies for Ca^{2+}, Mn^{2+}, and Zn^{2+} are 6.1, 11.5, and 14.3 kcal mol^{-1}, respectively. There are no experimental enthalpy data except for Mn^{2+},[12] but it

---

(18) Hase, W. L.; Feng, D.-F. *J. Chem. Phys.* **1981**, *75*, 738–744.

(19) Swaddle, T. W.; Merbach, A. E. *Inorg. Chem.* **1981**, *20*, 4212–4216.

(20) Swaddle, T. W.; Merbach, A. E. *Inorg. Chem.* **1981**, *20*, 4212.

is clear that the order of activation energies is $Zn^{2+} \simeq Mn^{2+} \gg Ca^{2+}$.[21] This is in reasonable agreement with the theory, particularly when it is realized that the activation entropies should be large positive for Zn^{2+}, small for Mn^{2+}, and large negative for Ca^{2+}. In terms of dielectric continuum theory, i.e. Born theory or modifications thereof, one would expect differences in ΔH_s(ts) and ΔH_s(oct) to be small although size differences between transition state and octahedral ground state might imply that any lowering of activation energy would be larger for Zn^{2+} than for Ca^{2+}.

Recent molecular-dynamics calculations have led to a much greater understanding of the detailed structural and dynamic aspects of water molecules in the vicinity of an ion. However, in order to solve the equations of motion accurately, it is necessary to use a very short time step (2×10^{-16} s) and this clearly limits the total time scale to a few picoseconds, much shorter than the time scale of solvent exchange. In order to study such chemical processes, it is necessary to equilibrate the system with the ion and its near neighbors fixed close to a plausible transition-state structure and then to study the return to equilibrium once the constraints are removed. This has yet to be done for aqueous electrolyte solutions.

The recent work of Heinzinger and co-workers on Mg^{2+}[22-24] clearly shows that the number of water molecules in the first hydration shell is exactly six and during the 3.3 ps of the simulation there was no exchange as expected. Their estimates of the simultaneous occupancy of octahedral sites and of various angular correlations clearly indicate octahedral coordination although it is apparently easily distorted. This agrees with our results that energies are relatively insensitive to small distortions and is also borne out by the very low-frequency Raman lines for the symmetric stretching vibration of aquated cations.[25] More significant to this work is the existence of a well-defined second shell containing 15 or so molecules that are still preferentially oriented with respect to the ion. It is clear that this second solvation shell will affect the energies of both the transition state and the ground state. The failure of our approach to give a reasonable transition-state structure for Zn^{2+} with the angle θ unconstrained is almost certainly due to neglect of second-shell effects, which can stabilize the exchanging water molecules that are well removed from the ion.

Acknowledgment. We acknowledge the Natural Sciences and Engineering Research Council of Canada for support for this work.

Registry No. H_2O, 7732-18-5; $Cu(H_2O)_6^{2+}$, 17787-72-3; $Mn(H_2O)_6^{2+}$, 15365-82-9; $Zn(H_2O)_6^{2+}$, 15906-01-1.

---

[21] Burgess, J. "Metal Ions in Solutions"; Ellis Harwood: Chichester, England, 1978; Chapter 11.

[22] Dietz, W.; Riede, W. O.; Heinzinger, K. *Z. Naturforsch., A* **1982**, *37A*, 1038-1048.

[23] Palinkas, G.; Radnai, T.; Dietz, W.; Szasz, Gy. I.; Heinzinger, K. *Z. Naturforsch. A* **1982**, *37A*, 1049-1060.

[24] Szasz, Gy. I.; Dietz, W.; Heinzinger, K.; Palinkas, G.; Radnai, T. *Chem. Phys. Lett.* **1982**, *92*, 388-392.

[25] Irish, D. E.; Jarv, T. *Faraday Discuss. Chem. Soc.* **1977**, *No. 64*, 95-101.

Notes

Contribution from the Dipartimento di Chimica,
Università di Venezia, 30123 Venice, Italy

Preparation and Properties of New Pentacoordinate Iron Nitrosyl Complexes

Gabriele Albertin and Emilio Bordignon*

Received December 19, 1983

Our interest in the chemistry of the nitrosyl complexes has been mainly devoted to the use of monodentate phosphite as coligand, and in this context, the syntheses of pentacoordinate $\{Co(NO)\}^8$ complexes[1] of the type $[CoXL_3(NO)]^+$ and $[CoL_4(NO)]^{2+}$ have recently been reported.[2] Similar investigations carried out on iron(II) halides by using gaseous NO allowed us to obtain new pentacoordinate $[FeL_4(NO)]^+$ (L = phosphite) derivatives, which are described in the present report. Furthermore, whereas some iron nitrosyl compounds also containing CO have been described,[3] no example of isocyanide–phosphine derivatives known to us has yet been reported. Therefore, in this paper we also present the reactivity of the $[FeL_4(NO)]^+$ species with isocyanides, leading to the synthesis of the first nitrosyl isocyanides–phosphite mixed-ligand complexes.

Results and Discussion

Nitric oxide reacts at room temperature with FeX_2 (X = Cl, Br) solutions containing an excess of phosphite to give the pentacoordinate nitrosyl $[FeL_4(NO)]^+$ (L = $P(OMe)_3$, $P(OEt)_3$) complexes.[4]

If the reaction is carried out employing a bulky ligand such as $PPh(OEt)_2$ or $P(O\text{-}i\text{-}Pr)_3$, only intractable oils are obtained, whose infrared spectra do not show in the NO stretching region bands attributable to the $[FeL_4(NO)]^+$ species. Therefore, only with phosphites of little steric hindrance does the reaction proceed, to give the $\{Fe(NO)\}^8$ complexes that were isolated and characterized.[5]

Selected properties of the new $[FeL_4(NO)]^+$ compounds are reported in Table I. They are stable both in the solid state

---

[1] The nitrosyl complexes have been classified according to the $\{M(NO)\}^n$ nomenclature: Enemark, J. H.; Feltham, R. D. *Coord. Chem. Rev.* **1974**, *13*, 339; *Top Stereochem.* **1981**, *12*, 155.

[2] (a) Albertin, G.; Bordignon, E.; Canovese, L.; Orio, A. *Inorg. Chim. Acta* **1980**, *38*, 77. (b) Albertin, G.; Bordignon, E.; Mazzocchin, G.; Orio, A.; Seeber, R. *J. Chem. Soc., Dalton Trans.* **1981**, 2127. (c) Albertin, G.; Pelizzi, G.; Bordignon, E. *Inorg. Chem.* **1983**, *22*, 515 and references therein.

[3] (a) Johnson, B. F. G.; Segal, J. A. *J. Chem. Soc., Dalton Trans.* **1972**, 1268. (b) Dolcetti, G.; Busetto, L.; Palazzi, A. *Inorg. Chem.* **1974**, *13*, 222. (c) Carrol, E. W.; Deeney, F. A.; Lalor, F. J. *J. Chem. Soc., Dalton Trans.* **1974**, 1430. (d) Baker, P. K.; Broadley, K.; Connelly, N. G. *J. Chem. Soc., Chem. Commun.* **1980**, 775. (e) Touchard, D.; Le Bozec, H.; Dixneuf, P. *Inorg. Chim. Acta* **1979**, *33*, L141. (f) Roustan, J. L. A.; Forgues, A. *J. Organomet. Chem.* **1980**, *184*, C13.

[4] From the reaction of FeX_2 with phosphites, we were able to isolate only the $[FeBrL_5]^+$ cation, which quickly reacted with NO to give the dinitrosyl $[FeL_2(NO)_2]$ as the main product. Only a small amount of $[FeL_4(NO)]^+$ was observed. The $[FeL_2(NO)_2]$ complex has been prepared by an alternative procedure: Kruck, T.; Waldmann, J.; Hoefler, M.; Birkenhaeger, G.; Odenbrett, C. *Z. Anorg. Allg. Chem.* **1973**, *402*, 16.

[5] (a) The previously reported complexes $[FeL_2(NO)]^+$ (L = 1,2-bis(diphenylphosphino)ethane) and $[FeL(NO)]^+$ (L = (2,2,2-tris(diphenylphosphino)ethyl)amine) have been obtained with bi- or tetradentate phosphine ligands. See ref 3a. (b) Hoffman, P. R.; Miller, J. S.; Ungermann, C. B.; Caulton, K. J. *J. Am. Chem. Soc.* **1973**, *95*, 7902. (c) Di Vaira, M.; Ghilardi, C. A.; Sacconi, L. *Inorg. Chem.* **1976**, *15*, 1555.